Effects of the microstructural uncertainties on the poroelastic and the diffusive properties of mortar

Adrien Socié, Yann Monerie, Frédéric Péralès

OVERLAY

Journal of Theoretical, Computational and Applied Mechanics

JTCAM

DIAMOND OPEN ACCESS

Identifiers
DOI 10.46298/jtcam.8849
OAI hal-03478716v3

History
Received Dec 15, 2021
Accepted Apr 25, 2022
Published Jun 20, 2022

Associate Editor
Anna Pandolfi

Reviewers
Anonymous
Anonymous

Open Review
OAI hal-03682105

Effects of the microstructural uncertainties on the poroelastic and the diffusive properties of mortar

Adrien Socié[1,3], Yann Monerie[2,3], and Frédéric Perales[1,3]

[1] Institut de Radioprotection et de Sureté Nucléaire (IRSN), PSN-RES/SEMIA/LSMA, BP3, Saint-Paul-lez-Durance, 13115, France
[2] Laboratoire de Mécanique et Génie Civil, University of Montpellier, CNRS, Montpellier, France
[3] MIST Laboratory, University of Montpellier, CNRS, IRSN, France

The assessment of the durability of civil engineering structures subjected to several chemical attacks requires the development of chemo-poromechanical models. The mechanical and chemical degradations depend on several factors such as the initial composition of the porous medium. A multi-scale model is used to incorporate the multi-level microstructural properties of the mortar material. The present paper aims to study the effect of morphological and local material properties uncertainties on the poroelastic and diffusive properties of mortar estimated with the help of analytical homogenization. At first, the proposed model is validated for different cement paste and mortar by comparison to experimental results and micromechanical models. Secondly, based on a literature study, sensitivity and uncertainty analysis have been developed to assess the stochastic predictions of the multi-scale model. The main result highlights the predominant impact of the cement matrix phases (C-S-H) and interfacial transition area at the mortar scale. Furthermore, the sensitive analysis underlines that the material properties induce more variability than the volume fraction.

Keywords: microporomechanics, homogenization, global sensitivity analysis, interfacial transition zone, mortar, Sobol variance decomposition

1 Introduction

The behavior of concrete is a topic of great concern in the context of the durability of civil engineering structures. The solicitations induced by the environment lead to the mineralogical evolution and delayed deformation of the concrete. The kinetic and the amplitude of the degradation depend on the properties and mineralogy of the mature cementitious material. For example, several works bring out the effect of the initial water-cement ratio on the concrete delayed deformation and chemical reactions, such as for sulfate attack (El-Hachem et al. 2012; Planel et al. 2006; Socié 2019), calcium leaching (Heukamp 2003; Stora et al. 2009) or drying shrinkage (Tognevi 2012). The water-cement ratio affects the cement paste composition and its porosity and thus modifies the overall poroelastic and diffusive properties of the material.

To consider the effect of the morphological multi-scale properties on the mechanical and chemical responses of concrete under different loading, analytical and numerical models have been developed (Bary 2008; Bernard and Kamali-Bernard 2012; Stora et al. 2009). The material properties of mature concrete based on multiscale models are performed in two steps: first, the microstructure properties, such as volume fraction of inclusions or phases' assemblage, are estimated, then, a micromechanical model is employed (Bary 2008; Bernard and Kamali-Bernard 2012; Honorio et al. 2016; Göbel et al. 2017; Stora et al. 2009; Venkovic et al. 2013). At cement scale, the volume fraction of hydrates and the capillary porosity are estimated by a hydration model. (Bary 2008; Honorio et al. 2016; Göbel et al. 2017; Stora et al. 2009; Venkovic et al. 2013) and at mortar or concrete scale, an additional function is considered to estimate the volume fraction of the so-called Interfacial Transition Zone (ITZ) between the matrix and the inclusions (Garboczi

and Bentz 1997; Honorio et al. 2016). Each model depends on a wide variety of parameters (size of the inclusions, clinker composition...) that affect the estimated volume fraction and thus the macroscopic property (Honorio et al. 2016; Göbel et al. 2017; Venkovic et al. 2013). Furthermore, multi-scale models are function of the material properties of each considered phase. These properties are dependent on experimental measurement (Constantinides and Ulm 2004; Haecker et al. 2005), on post-processing used (i.e. inverse analysis) (Hashin and Monteiro 2002; Seigneur et al. 2017) or molecular simulations results (Jelea 2018; Hajilar and Shafei 2015; Honorio et al. 2020b).

Therefore, a large number of parameters are required and their inherent uncertainty influences the overall predicted properties. Uncertainty and sensitivity analysis have already been carried out to quantify the stochastic variation due to hydration models and material properties from nanoscale to macroscale (concrete) (Göbel et al. 2017; Honorio et al. 2020a; Sudret et al. 2010; Venkovic et al. 2013). Göbel et al. (2017) reveal that the uncertainty due to the input parameters is magnified during the upscaling processes and uncertainties of inclusion properties take a major role in the overall elastic variation. Göbel et al. (2017) and Venkovic et al. (2013) determine the overall uncertainties of the hydration processes through the effects of the parameters. Göbel et al. (2017) show the effect of the hydration model uncertainties increases with the number of input parameters. Göbel et al. (2017) and Venkovic et al. (2013) highlight that the elastic parameters have the most significant impact on the variability of the homogenized poroelastic properties. These works mostly focus on the elastic properties except Venkovic et al. (2013) who have studied the poroelastic properties but only at the cement scale. Honorio et al. (2020a) have studied the variability of the response obtained with an analytical homogenization model in order to obtain the concrete's electrical properties. The multiscale model gives the electrical value from the C-S-H to the concrete scale. The electrical conductivity homogenization scheme is similar to the one of the diffusion and following diffusion assumption, the electrical conductivity only occurs in the pore solution. The propagation of the Monte-Carlo simulation applied to a micromechanical model led to the study of the impact of the uncertainties across each scale induced by the pore conductivity variability.

The works previously mentioned are dedicated to the uncertainties of the analytical homogenization model applied to the estimation of the poroelastic or conductivity properties. The model developed in this study allows to estimate the poroelastic and diffusive properties of mortar used to simulate the chemo-poromechanical behavior of concrete submitted to chemical attacks (Socié et al. 2019; Socié et al. 2021). The work mainly focuses on two aspects: the effect of the ITZ material properties and volume fraction, and the effect of the uncertainties relative to the clinker composition. Note that, to our knowledge, theses aspects have never been studied in the literature before. The first point has been driven by the lack of information relative to the interfacial zone even though multiscale models consider its effects (Patel et al. 2016). Indeed, as described in (Honorio et al. 2020a), even though the ITZ plays a major role in the efficient mortar properties, and multiscale approaches should be taken into account (Hashin and Monteiro 2002; Heukamp 2003; Honorio et al. 2016; Sun et al. 2007), the challenge rests on knowing its volume fraction and its composition. The second point is based on the study of Stutzman et al. (2014) that shows that the Bogue constant (Bogue 1929; Taylor 1989) introduces uncertainties that can have a significant effect on the cement paste microstructure estimated by hydration models. A part of the study focuses on the impact of these uncertainties instead of the uncertainties relative to the hydration model such as developed in (Göbel et al. 2017; Honorio et al. 2020a; Venkovic et al. 2013). The study presented in this article has been also extended to the main uncertainties relative to the hydrate's properties. Finally, the identification of the main contributor to the output variation and their interactions has been carried out by a sensitivity analysis.

This paper begins with a description of the microporomechanics model (Section 2). Section 3 is dedicated to its validation. The impact of the main variable in the homogenized properties is underlined. The uncertainties of the material properties and microstructure parameters are studied in Section 4. At first, each uncertainty is studied separately to exhibit the most predominant parameters. The study highlights the main effect of the cement paste matrix, C-S-H, and ITZ to respectively the cement paste and mortar variation. Secondly, the global uncertainties are presented for three mortars distinguished by their water-cement ratios: 0.3, 0.4 and 0.5.

The main results show that the uncertainty increases with the upscaling and the predominant impacts of the ITZ characteristic on the chemo-mechanical mortar properties. A Sobol variance decomposition is studied in Section 5 to highlight the impact of the main input variable and their interactions.

2 Microporomechanical model

The multi-scale model permits the estimation of the poroelastic parameters and the diffusion coefficient of the chemo-poromechanical model developed in (Socié 2019; Socié et al. 2019). The model is dedicated to the study of geomaterial expansion due to the strong precipitation of a solid inside the porous medium. The chemical software describes the mineralogy evolution and the poromechanical model estimates the swelling by the volume fraction of the main precipitated solid, denoted φ_{ms}. The porous medium is described with an isotropic elastic poromechanical model, where the pressure depends on the volume fraction of the main precipitated solid and the strain tensor (Socié 2019; Socié et al. 2019):

$$\begin{cases} \boldsymbol{\sigma} = \mathbb{C} : \boldsymbol{\varepsilon} - bP\boldsymbol{I} \\ P = N\langle \varphi_{\text{ms}} - \langle \varphi_{\text{ms}}^0 + b \operatorname{tr} \boldsymbol{\varepsilon} \rangle_+ \rangle_+ \end{cases} \tag{1}$$

where $\boldsymbol{\sigma}$ is the Cauchy stress tensor [Pa], $\mathbb{C}$ is the fourth order stiffness tensor [Pa], $\boldsymbol{\varepsilon}$ is the linearized strain tensor, P is the pore pressure [Pa], $\boldsymbol{I}$ is the identity second order tensor, b is the Biot coefficient assuming overall isotropy [−], N is the Biot skeleton modulus [Pa], $\langle x \rangle_+ = (x + |x|)/2$ are the Macaulay brackets, and φ_{ms}^0 represents the quantity of initial pores to be filled by the solid to induce swelling [−].

The microporomechanical model aims to estimate the following mortar variables from the microstructure:

- the Biot coefficient b_{m} and Biot skeleton modulus N_{m},
- the bulk and shear moduli, k_{m} and g_{m}, and thus the Young modulus E_{m} and the Poisson ratio ν_{m},
- the diffusion coefficient D_{m}.

The subscript m defines the phase of the mortar material. The Biot parameters are obtained considering that the minerals inducing the pore pressure precipitate in the capillary pores and the pores of the mortar's Interfacial Transition Zone.

Section 2.2 describes the homogenization function based on a multi-scale representativity detailed in Section 2.1.

2.1 Description of the mortar microstructure

We consider a two-scale modeling illustrated in Figure 1:

Level I: cement paste The Portland cement paste (CEM I) is a material with an isotropic matrix, called C-S-H, containing inclusions assumed spherical and randomly distributed in space. The inclusions correspond to the capillary porosity, the unhydrated cement and the main solid hydrated phases: portlandite, ettringite, and an AFm phase which can be katoite, hydrogarnet or monosulfoaluminate. Depending on the hydration model, the unhydrated cement is taken into account.

Level II: mortar scale Mortar is a three-coated sphere assemblage with an isotropic matrix (cement paste) containing inclusions randomly distributed in space and in orientation (sand) and a percolation phase called the Interfacial Transition Zone (ITZ).

The C-S-H phase can be described as a porous medium with two types of C-S-H characterized by their densities. The C-S-H density affects the mechanical and diffusive properties (Béjaoui and Bary 2007; Constantinides and Ulm 2004; Stora et al. 2009; Tennis and Jennings 2000; Ulm et al. 2004) and models have different cement paste representations or consider a dedicated representation for the C-S-H scale (Bary et al. 2014; Béjaoui et al. 2006; Honorio et al. 2016; Göbel et al. 2017; Venkovic et al. 2013; Ulm et al. 2004). Furthermore, some studies (Honorio et al. 2016; Stora et al. 2009) consider a representation of the ITZ phase whereas Hashin and Monteiro (2002); Heukamp (2003) estimate its properties from the cement paste value. Since the microstructure

and the associated coefficients of C-S-H and ITZ are difficult to obtain, we choose to not describe their microstructures. Their coefficients are obtained with a probabilistic distribution function.

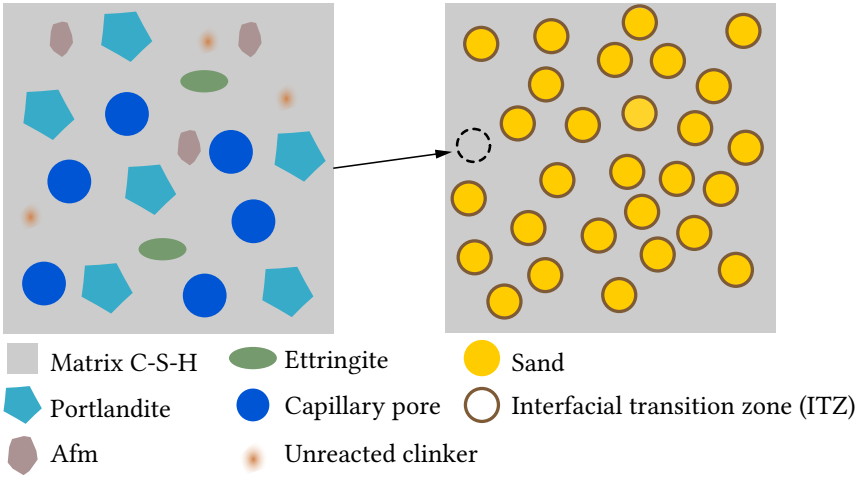

Figure 1 Multiscale heterogeneous microstructure of mortar, inclusions are assumed spherical.

2.2 Estimation of the chemo-poromechanical properties

The homogenization schemes follow the recommendations of the literature for a mature material and are similar for mechanical and diffusive properties:

Cement paste Mori-Tanaka scheme (Mori and Tanaka 1973) used in (Bary 2008; Heukamp 2003; Venkovic et al. 2013; Ulm et al. 2004; Le 2011),

Mortar Generalized Self-Consistent scheme (Hashin and Monteiro 2002) used in (Bary and Béjaoui 2006; Tognevi 2012; Stora et al. 2009).

Note that the Mori-Tanaka scheme is not suitable for early-age concrete when there is not enough C-S-H to consider this phase as a matrix. Our model is applied to mature material and cement paste admitting a high hydration rate.

2.2.1 Cement paste

The cement paste is assumed to be composed of N^{ph} phases: N^{sol} solid phases and capillarity pores, contained in a matrix of C-S-H. We consider that all inclusions are spherical. The bulk k_{cp} and shear g_{cp} moduli depend on the volume fraction φ_{i}, shear modulus g_i and bulk modulus k_i of phase i such that

$$k_{\text{cp}} = \frac{k_{\text{csh}} + \dfrac{4g_{\text{csh}}}{3}\displaystyle\sum_{i=1}^{N^{\text{ph}}} \varphi_{\text{i}} \frac{k_i - k_{\text{csh}}}{k_i + 4/3g_{\text{csh}}}}{1 - \displaystyle\sum_{i=1}^{N^{\text{ph}}} \varphi_{\text{i}} \frac{k_i - k_{\text{csh}}}{k_i + 4/3g_{\text{csh}}}}, \quad g_{\text{cp}} = \frac{g_{\text{csh}} + H_{\text{csh}}\displaystyle\sum_{i=1}^{N^{\text{ph}}} \varphi_{\text{i}} \frac{g_i - g_{\text{csh}}}{g_i + H_{\text{csh}}}}{1 - \displaystyle\sum_{i=1}^{N^{\text{ph}}} \varphi_{\text{i}} \frac{g_i - g_{\text{csh}}}{g_i + H_{\text{csh}}}}, \tag{2}$$

and $H_{\text{csh}} = g_{\text{csh}}(3/2k_{\text{csh}} + 4/3g_{\text{csh}})/(k_{\text{csh}} + 2g_{\text{csh}})$ where the subscripts "csh" and "cp" denote C-S-H and cement paste respectively.

We assume that the solid, called here "main precipitated solid φ_{ms}", see Equation (1), inducing the macroscopic swelling precipitates in the capillarity porosity and ITZ porosity (Socié et al. 2021; Socié 2019). Accordingly, we do not consider the C-S-H poroelastic properties. In that way, the Biot tensor $b_{\text{cp}}\boldsymbol{I}$ and Biot skeleton modulus N_{cp} of the cement paste only depend on the hydrostatic part of the localization tensor A_i^h (Ulm et al. 2004):

$$b_{\text{cp}}\boldsymbol{I} = \left[1 - \sum_{i=1}^{N^{\text{sol}}} \varphi_{\text{i}} A_i^h\right]\boldsymbol{I}, \quad \frac{1}{N_{\text{cp}}} = \sum_{i=1}^{N^{\text{sol}}} \frac{\varphi_{\text{i}}(1 - A_i^h)}{k_i} \tag{3}$$

with

$$A_i^h = \left(1 + \frac{3k_{\text{csh}}}{3k_{\text{csh}} + 4g_{\text{csh}}}\left(\frac{k_i}{k_{\text{csh}}} - 1\right)\right)^{-1}\left[\sum_i^{N^{\text{ph}}} \varphi_{\text{i}}\left(1 + \frac{3k_{\text{csh}}}{3k_{\text{csh}} + 4g_{\text{csh}}}\left(\frac{k_i}{k_{\text{csh}}} - 1\right)\right)^{-1}\right]^{-1}. \tag{4}$$

The effective diffusion coefficient D_{cp} of the cement paste depends on the diffusion of the phases (Dormieux et al. 2006):

$$D_{\text{cp}} = D_{\text{csh}}\frac{1 + 2\sum_i \varphi_{\text{i}}\dfrac{D_i - D_{\text{csh}}}{D_i + 2D_{\text{csh}}}}{1 - \sum_i \varphi_{\text{i}}\dfrac{D_i - D_{\text{csh}}}{D_i + 2D_{\text{csh}}}}. \tag{5}$$

Moreover, we assume that the capillary porosity and the C-S-H are the only diffusive phases (Bary et al. 2014; Bary and Béjaoui 2006; Bogdan 2015; Stora et al. 2009).

2.2.2 Mortar

The mortar is mainly represented as a three-coated sphere assemblage where the Generalized Self-Consistent scheme is used in order to take into account the ITZ phase as an interphase coating of the aggregate particle. The mortar properties depend on the ITZ, the sand and the cement paste properties. In this section, the subscripts "itz" and "s" define the ITZ and sand, respectively. The bulk modulus is defined by (Hashin and Monteiro 2002; Nguyen et al. 2011; Tognevi 2012)

$$k_{\text{m}} = k_{\text{cp}} + \frac{\varphi_{\text{s}} + \varphi_{\text{itz}}}{\dfrac{1}{k^* - k_{\text{cp}}} + \dfrac{3\varphi_{\text{cp}}}{3k_{\text{itz}} + 4g_{\text{itz}}}} \tag{6}$$

with $k^* = k_{\text{itz}} + (\varphi_{\text{s}}/(\varphi_{\text{s}} + \varphi_{\text{itz}}))/(1/(k_{\text{s}} - k_{\text{itz}}) + 3\varphi_{\text{itz}}/(\varphi_{\text{s}} + \varphi_{\text{itz}})/(3k_{\text{itz}} + 4g_{\text{itz}}))$. The shear modulus is deduced from an implicit system depicted in (Hashin and Monteiro 2002; Nguyen 2010; Socié 2019). For a sake of compactness, we refer the reader to these papers for details. The Biot coefficient and skeleton modulus depend on poroelastic phases values (Bary and Béjaoui 2006; Nguyen et al. 2011):

$$b_{\text{m}} = b_{\text{cp}} + \frac{(3k_{\text{cp}} + 4g_{\text{cp}})(1 - \varphi_{\text{cp}})[(b_{\text{itz}} - b_{\text{cp}})(4g_{\text{itz}}(1 - \varphi_{\text{cp}}) + 3k_1^*) - \varphi_{\text{s}}(b_{\text{itz}} - 1)(3k_{\text{itz}} + 4g_{\text{itz}})]}{9k_s k_{\text{itz}}\varphi_{\text{cp}}(1 - \varphi_{\text{cp}}) + 12g_{\text{itz}}k_2^*\varphi_{\text{cp}} + (4g_{\text{cp}} + 3k_{\text{cp}}(1 - \varphi_{\text{cp}}))(4g_{\text{itz}}(1 - \varphi_{\text{cp}}) + 3k_1^*)} \tag{7}$$

with $k_1^* = k_{\text{itz}}\varphi_{\text{s}} + k_s\varphi_{\text{itz}}$ and $k_2^* = k_s\varphi_{\text{s}} + k_{\text{itz}}\varphi_{\text{itz}}$, and

$$\begin{aligned}
\frac{1}{N_{\text{m}}} &= \frac{\varphi_{\text{s}} + \varphi_{\text{itz}}}{N^*} + \frac{\varphi_{\text{cp}}}{N_{\text{cp}}} + \frac{3(b^* - b_{\text{cp}})^2\varphi_{\text{s}}(\varphi_{\text{s}} + \varphi_{\text{itz}})}{3(\varphi_{\text{s}} + \varphi_{\text{itz}})(k_{\text{cp}} - k^*) + 3k^* + 4g_{\text{cp}}} \\
\frac{1}{N^*} &= \frac{\varphi_{\text{s}}/(\varphi_{\text{s}} + \varphi_{\text{itz}})}{N_s} + \frac{1 - \varphi_{\text{s}}/(\varphi_{\text{s}} + \varphi_{\text{itz}})}{N_{\text{itz}}} + \frac{3(b_{\text{itz}} - b_s)^2(1 - \varphi_{\text{s}}/(\varphi_{\text{s}} + \varphi_{\text{itz}}))\varphi_{\text{s}}/(\varphi_{\text{s}} + \varphi_{\text{itz}})}{3\varphi_{\text{s}}(k_{\text{itz}} - k_s)/(\varphi_{\text{s}} + \varphi_{\text{itz}}) + 3k_s + 4g_{\text{itz}}} \\
b^* &= b_{\text{itz}} + \frac{(3k_{\text{itz}} + 4g_{\text{itz}})(b_{\text{m}} - b_{\text{itz}})\varphi_{\text{s}}/(\varphi_{\text{s}} + \varphi_{\text{itz}})}{4g_{\text{itz}} + 3k_s(1 - \varphi_{\text{s}}/(\varphi_{\text{s}} + \varphi_{\text{itz}}) + 3k_{\text{itz}}\varphi_{\text{s}}/(\varphi_{\text{s}} + \varphi_{\text{itz}}))}.
\end{aligned} \tag{8}$$

The sand is considered nonreactive with a negligible diffusion coefficient. Based on (Bogdan 2015; Heukamp 2003; Hashin and Monteiro 2002; Salah et al. 2019), elastic and diffusive properties of ITZ are deduced from the cement paste coefficients. As a first approach, due to the high porosity of the ITZ phase and because the phase is mostly composed of matrix solid phases (Honorio et al. 2016), the poroelastic properties of the ITZ are estimated from a bimaterial representation (Dormieux et al. 2006):

$$b_{\text{itz}} = 1 - \frac{k_{\text{itz}}}{k_{\text{csh}}}; \quad \frac{1}{N_{\text{itz}}} = \frac{b_{\text{itz}} - \phi_{\text{itz}}}{k_{\text{csh}}}. \tag{9}$$

The diffusive coefficient of the mortar is estimated with the so-called three-coated sphere model (Bary and Béjaoui 2006; Stora et al. 2009):

$$D_{\text{m}} = D_{\text{cp}} + (1 - \varphi_{\text{cp}})\left[[D_{\text{itz}} - D_{\text{cp}} + D_1^*(D_2^*)^{-1}]^{-1} + \frac{\varphi_{\text{cp}}}{3D_{\text{cp}}}\right]^{-1} \tag{10}$$

with $D_1^* = \varphi_{\text{s}}/(\varphi_{\text{s}} + \varphi_{\text{itz}})$ and $D_2^* = (D_{\text{s}} - D_{\text{itz}})^{-1} + (1 - D_1^*)(3D_{\text{itz}})^{-1}$.

3 Validation

This section aims to validate this simple and closed-form model by comparison with a more sophisticated model (Stora et al. 2009) and the model's availability to capture the microstructure variation.

3.1 Impact of the microstructure evolution

The ability of the model to describe the microstructure evolution is depicted with the effect of the water-cement mass ratio on the overall properties. The cement paste microstructure is estimated by Bary and Béjaoui (2006); Tognevi (2012) and summarized in Table 1. As previously depicted,

w/c	Ettringite	AFm	Portlandite	Unreacted cement	C-S-H
0.3	0.074	0.072	0.152	0.137	0.494
0.35	0.075	0.072	0.156	0.094	0.507
0.4	0.072	0.073	0.155	0.064	0.509
0.45	0.069	0.073	0.151	0.043	0.504
0.5	0.065	0.075	0.144	0.03	0.494
0.6	0.058	0.068	0.131	0.014	0.48

Table 1 Cement paste composition (Bary and Béjaoui 2006; Tognevi 2012). We consider one C-S-H phase and its volume fraction is equal to the sum of the inner and the outer C-S-H volume fractions given in (Bary and Béjaoui 2006; Tognevi 2012). In the validation part, the AFm is modeled by the monosulfoaluminate. In the applications part, Sections 4 and 5, the AFm phase is represented by the katoite to be consistent with the chemo-poromechanical model (Socié 2019).

we consider one C-S-H phase and its volume fraction is estimated equal to the sum of the inner and the outer C-S-H volume fraction of (Bary and Béjaoui 2006; Tognevi 2012). The AFm is modeled by the monosulfoaluminate. The material properties are described in Table 2. The mechanical results agree well with the experimental measurements of Haecker et al. (2005) shown in Figure 2(a).

	D [m^2 s^{-1}]	E [GPa]	ν	References
C-S-H	4.64×10^{-12}	23.8	0.24	Constantinides and Ulm 2004; Venkovic et al. 2013, Table B.4
Portlandite	0	38	0.324	Haecker et al. 2005; Venkovic et al. 2013
Ettringite, Katoite	0	22.4	0.25	Haecker et al. 2005
Monosulfoaluminate	0	38	0.324	Haecker et al. 2005
Anhydrous cement	0	117.6	0.314	Haecker et al. 2005
Sand	0	62.4	0.21	Heukamp 2003
Capillary pore	$D_0 = 2 \times 10^{-9}$	0	0	Bogdan 2015
ITZ	$10.3 \times D_{\text{cp}}$	$0.175 \times E_{\text{cp}}$	ν_{cp}	Tables C.5 and C.6

Table 2 Material properties of mortar phases.

Figure 2(b) compares the diffusion coefficient to the experimental results reported in (Bary and Béjaoui 2006). The considered C-S-H diffusion coefficient is equal to 8×10^{-12} m^2 s^{-1} to fit the experimental result. The diffusion model can catch the effects of the microstructure and fits well the experimental results. Nevertheless, for a low water-cement ratio, the model overestimates the diffusion value due to the simplified representation of the C-S-H phases. As described in (Bary and Béjaoui 2006), the model needs to consider the influence of the water-cement ratio in the volume fraction of the different C-S-H phases (inner and outer).

3.2 Validation of the Micromechanical representation

In Table 3, the model is compared to the reference model of Stora et al. (2009) which has a microstructure representation of the C-S-H and the ITZ phases. The microstructure and the hydrated properties are taken from (Stora et al. 2009). In our model, the properties of the C-S-H and the ITZ phases are estimated by a stochastic model. The range of values are estimated using a Monte-Carlo experiments on 10000 samples to take into account the uncertainties associated

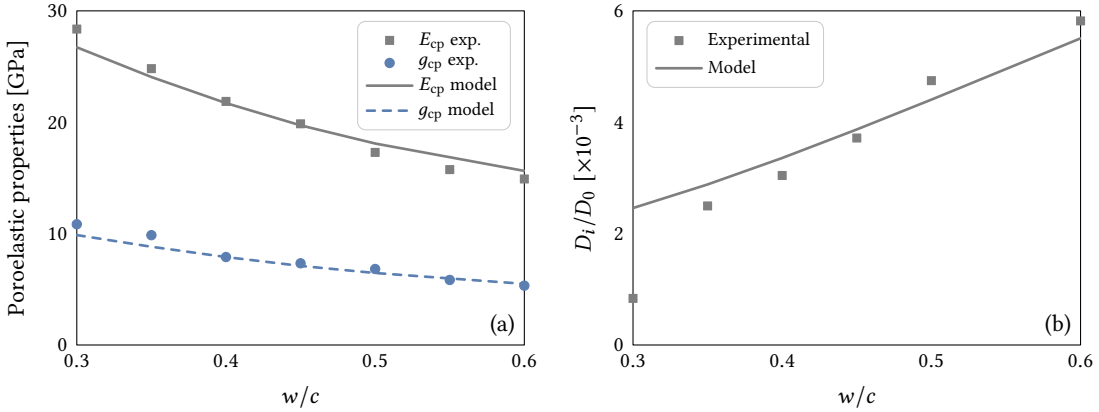

Figure 2 Effect of the water-cement ratio w/c on the material properties of cement paste: (a) elastic properties compared to the experimental results of Haecker et al. (2005) and (b) normalized diffusion properties compared to the experimental results of Bary and Béjaoui (2006).

Material	Parameters	Model	Stora et al. (2009)	Exp. data
Cement paste: Gallé et al. (2004)	Young Modulus	20.389 ± 1.1	23.7	23
Cement paste: Le Bellégo (2001), Le Bellégo et al. (2003)	Young Modulus Diffusion coefficient	23.58 ± 1.27 3.59 ± 1.97	25.65 3.2	
Mortar: Le Bellégo (2001), Le Bellégo et al. (2003)	Young Modulus Diffusion coefficient	39.45 ± 3.44 3.97 ± 2.55	38.5 1.8	38.2 1.7*

Table 3 Comparison of the micromechanical estimation of cement paste and mortar properties with experimental data (Le Bellégo 2001; Le Bellégo et al. 2003; Gallé et al. 2004) and analytical homogenization model (Stora et al. 2009). Young modulus in [GPa] and diffusion coefficient in [10^{-12} m^2 s^{-1}]. *Experimental value from (Stora et al. 2009) and measured by Bourdette (1994).

with the C-S-H and ITZ properties. The parameters are described by a log-normal distribution where the mean value and standard deviation parameters of the normal law distribution are respectively summarized in Tables 2 and 4. The diffusion and elastic properties fit well with the model and experimental results, except for the material of Gallé et al. (2004) where the model estimates a lower Young's modulus value.

Main results The model can both predict the poroelastic and diffusive properties from an estimated microstructure and capture the effects of the cement mineralogy in the overall behavior.

4 Uncertainty propagation

The propagation of uncertainty of the poroelastic and diffusive mortar properties are explored through a Monte-Carlo method. At first, each uncertainty is studied separately and divided into two domains: material properties, reported in Section 4.1, and microstructural characteristics, in Section 4.2. We consider a mortar composed of a CEM I cement paste, detailed in Table 1, with a water-cement ratio of 0.4, an ITZ volume fraction of 0.185 and a volume fraction of sand of 0.55. Each parameter is investigated independently, the others set to their mean value, see Tables 1 and 2. Secondly, we study the impact of the global uncertainties on three water-cement ratios: 0.3, 0.4 and 0.5. The study has been developed to simulate a sulfate attack where the aluminate phase is modeled by the katoite (Socié 2019). In that way, we assume that the AFm phase is represented by the katoite phase. Our results can be applied to a system where the aluminate is represented by the monosulfoaluminate. Indeed, recent molecular simulations (Honorio et al. 2020b) highlight that the elastic properties of monosulfoaluminate are similar to the ettringite and thus the katoite.

A Monte-Carlo study with 10 000 simulations by parameter is performed. In the sequel, the input parameters of the multi-scale model are described by log-normal distributions to ensure the

strict positivity:

$$p(x) = \frac{1}{xV\sqrt{2\pi}} \exp\left(-\left(\frac{\ln x - \overline{e}}{V\sqrt{2}}\right)^2\right), \tag{11}$$

where $\overline{e}$ and V are the mean and the standard deviation of the normal law distribution, respectively. For each study, the output mean and standard deviations are estimated.

Appendix A is dedicated to the estimation of the parameters uncertainties and summarizes the various coefficients used in the literature.

4.1 Uncertainty from the material properties

4.1.1 Input parameters

Solid uncertainties at cement paste scale At cement paste scale, the porous medium is affected by the uncertainties associated with the solid phases (hydrates). The global sensitivity analysis led by Venkovic et al. (2013) have shown that the poroelastic properties are essentially impacted by the properties of C-S-H and portlandite. Based on the work of Venkovic et al. (2013), we study the impact of the uncertainties of the Young Modulus of the two hydrates. For the diffusion part, the study is focused on the C-S-H phase. Indeed, in the analytical model benchmark led by Patel et al. (2016), the authors highlight that every tested multi-scale and empirical model has to fit the diffusion associated with the matrix phases that induce a wide variability of values (see Appendix B). This wide variability is explained by the difference in the microstructure representation and the fact that the calibration value depends on the experimental techniques used to obtain the cement paste diffusivity (Patel et al. 2016). Furthermore, the C-S-H's diffusion coefficient is difficult to identify because of the sorption reactions between the cation and anion in solution and the solid phases (Seigneur et al. 2017).

ITZ properties At mortar scale, the ITZ value mainly affects the poroelastic and diffusion properties (Heukamp 2003; Honorio et al. 2016). Tables C.5 and C.6 show the large variability in the literature. The values are generally estimated by inverse analysis (Heukamp 2003; Hashin and Monteiro 2002; Garboczi 1997; Patel et al. 2016) which depends both on the analytical homogenization/numerical scheme used and the experiment uncertainties (Aït-Mokhtar et al. 2013; Patel et al. 2016).

The input parameters are summarized in Table 4. The mean value and standard deviation

	D_{csh} [m^2 s^{-1}]	E_{csh} [GPa]	E_{ch} [GPa]	D_{itz} [m^2 s^{-1}]	E_{itz}
V	2.84×10^{-12}	2	5	$6.93 \times D_{cp}$	$0.175 \times E_{cp}$

Table 4 Standard deviation of the normal law distribution associated to the material properties uncertainties. The mean values are specified in Table 2.

of portlandite's Young modulus are identified from (Constantinides and Ulm 2004; Venkovic et al. 2013). The C-S-H value is estimated for water-cement ratios of 0.3 and 0.5 by analytical homogenization (Mori-Tanaka scheme) from the measurement of the uncertainties (Constantinides and Ulm 2004). The high and low-density C-S-H volume fractions are estimated from (Tennis and Jennings 2000). The mean value and standard deviation of the C-S-H diffusion and ITZ properties are estimated from the literature and presented in Appendices B and C.

4.1.2 Results

The results are reported in Table 5 and plotted in Figure 3. At cement scale, the C-S-H has the main uncertainties impact. In contrast to the results of Venkovic et al. (2013) and Göbel et al. (2017), the portlandite and C-S-H elastic properties do not have a strong impact on effective mortar properties. The mortar poroelastic properties are mainly affected by the uncertainties associated with the ITZ rigidity (strong input dispersion, see Table C.6) and the poroelastic properties of the transition zone (Nguyen et al. 2011). The uncertainties propagation from cement paste to the mortar admit a quite similar variance.

The diffusion coefficient has a larger variance than the elastic properties. First of all, the C-S-H uncertainties have a significant effect on the mortar and cement paste properties. The uncertainty propagation is stable and the mortar standard deviation is larger than cement paste one. This effect is undergone by the ITZ diffusion coefficient that is a function of the cement paste properties. At mortar level, the ITZ still plays a major role in the uncertainty but, instead of the poroelastic properties, there is a competition between the C-S-H and ITZ uncertainties on the mortar diffusion variation.

Uncertainties	E_{cp} [GPa]	E_m [GPa]	$b_m N_m$ [GPa]	D_{cp}/D_0 [$\times 10^{-3}$]	D_m/D_0 [$\times 10^{-3}$]
E_{csh}	21.36 (±1.2)	37.43 (±1.01)	25.07 (±0.7)	–	–
E_{ch}	21.35 (±0.4)	37.45 (±0.31)	25.04 (±0.56)	–	–
E_{itz}/E_{cp}	–	36.66 (±5.01)	26.42 (±18.11)	–	–
D_{csh}	–	–	–	1.93 (±1.05)	3.09 (±1.69)
D_{itz}/D_{cp}	–	–	–	–	2.99 (±1.28)

Table 5 Effect of the material properties uncertainties on the homogenized properties.

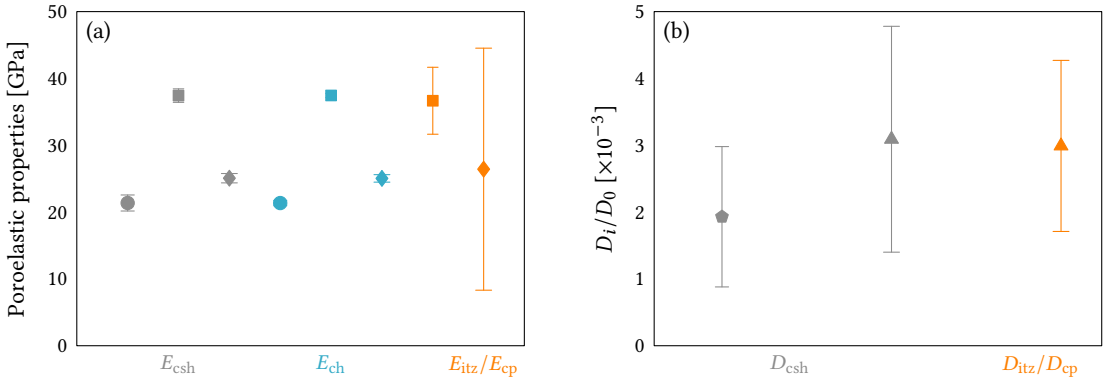

Figure 3 Uncertainty propagation from the material properties. Mean value and standard deviation obtained through Monte-Carlo simulation are respectively represented by data symbols and error bars: (a) poroelastic properties and (b) normalized diffusion properties. Legend: ●E_{cp}, ■E_m, ♦$b_m N_m$, ⬟D_{cp}/D_0, and ▲D_m/D_0.

The C-S-H and ITZ have the main uncertainties impact respectively at cement paste and mortar scales. Only for the diffusion coefficient, the C-S-H uncertainties play a major role in the global mortar variance.

4.2 Uncertainty from the microstructure

4.2.1 Input parameters

We consider two main impacts of the microstructure in each level: the hydrate volume fraction and the ITZ volume fraction.

Hydrate volume fraction Most of the hydration models (Buffo-Lacarrière et al. 2007; Papadakis et al. 1991; Jennings and Tennis 1994; Tennis and Jennings 2000) are based on the alite, belite, aluminate and ferrite mass fractions estimated from the chemical clinker composition by Bogue's formula (Bogue 1929; Taylor 1989). Stutzman et al. (2014) highlighted that the Bogue constant introduces a significant uncertainty that mainly impacts the alite and belite mass fractions (around 10 %) and thus the portlandite and C-S-H volume fractions. Furthermore, we notice a strong variability of C-S-H molar volume in the literature: for a calcium silica ratio of 1.65, the molar volume is equal to 0.084 L mol^{-1} (Planel 2002) or 0.078 L mol^{-1} (Lothenbach et al. 2019). This variability impacts the overall properties estimated by the hydration-homogenization model (Socié 2019). In order to capture both the impact of Bogue's constant and molar volume uncertainties in the microstructure properties, a Monte-Carlo study is carried out using the hydration model of Socié (2019), see Appendix A. The associated standard deviations are applied to the studied microstructures, as reported in Table 6. The variation of the solid volume fraction

impacts the overall properties through the capillary porosity

$$\phi = 1 - \sum_{i}^{N^{\text{sol}}} \varphi_{\text{i}}. \tag{12}$$

	Cement paste level				Mortar level	
	φ_{csh}	φ_{ch}	φ_{ett}	φ_{kat}	φ_{itz}	$\phi_{\text{itz}}/\phi_{\text{cp}}$
V	0.018	0.005	0.007	0.011	0.071	0.25

Table 6 Standard deviation of the normal law distribution associated to the microstructural properties uncertainties. The mean values are specified in Table 1 for $w/c = 0.4$ and ITZ volume fraction of 0.185. The subscripts 'kat' and 'ett' respectively define the values associated with the katoite and ettringite.

ITZ volume fraction The ITZ volume fraction depends on the sand granulometry (Garboczi and Bentz 1997), the sand mean size particle (Garboczi and Bentz 1997), the hydration rate (Sun et al. 2007), the inclusion properties (Keinde 2014) and the water cement ratio (Sun et al. 2007; Tognevi 2012). The ITZ volume fraction is usually estimated from the particle size distribution of sand and considering a constant ITZ thickness by Garboczi's formula (Garboczi and Bentz 1997), such as (Heukamp 2003; Honorio et al. 2016; Stora et al. 2009; Tognevi 2012). The great uncertainty of ITZ thickness influences the estimation of the volume fraction (Honorio et al. 2016; Honorio et al. 2020a). The mean value and the standard deviation are deduced from the volume fractions used in the literature and summarized in Table C.7. The variation of the ITZ volume fraction impacts the cement paste volume fraction and satisfies $\varphi_{\text{cp}} = 1 - \varphi_{\text{itz}} - \varphi_{\text{s}}$.

Finally, to study the influence of the ITZ porosity on the poroelastic properties (9), an uncertainty analysis is carried out with the mean value of ϕ_{itz}/ϕ equals to 1.75 and a standard deviation of 0.25, based on the global values used in the literature, see Table C.8.

4.2.2 Results

The results are presented in Table 7 and plotted in Figure 4.

Uncertainties	E_{cp} [GPa]	E_{m} [GPa]	$b_{\text{m}}N_{\text{m}}$ [GPa]	$D_{\text{cp}}/D_0 \times 10^3$	$D_{\text{m}}/D_0 \times 10^3$
φ_{csh}	21.39 (±0.78)	37.46 (±0.66)	25.14 (±2.03)	1.95 (±0.11)	3.14 (±0.18)
φ_{ch}	21.38 (±0.26)	37.47 (±0.23)	25.07 (±0.44)	1.95 (±0.05)	3.13 (±0.07)
φ_{ett}	21.39 (±0.29)	37.48 (±0.25)	25.06 (±0.78)	1.95 (±0.06)	3.13 (±0.1)
φ_{kat}	21.39 (±0.46)	37.48 (±0.39)	25.06 (±1.23)	1.95 (±0.1)	3.13 (±0.16)
φ_{itz}	–	37.65 (±2.76)	24.91 (±2.95)	–	3.13 (±0.8)
$\phi_{\text{itz}}/\phi_{\text{cp}}$	–	–	25.26 (±2.37)	–	–

Table 7 Impact of the microstructural properties uncertainties on the homogenized properties.

At cement paste scale, the variations of poroelastic properties and diffusion coefficient increase with the volume fraction uncertainties. This effect is due to two aspects. First of all, the Young modulus of each hydrate remains similar and we do not consider their diffusivity, see Table 2. Secondly, the porosity is linearly dependent on the volume fraction (12). Because the katoite is the hydrate inclusion (excluding C-S-H) that admits the larger volume fraction uncertainty, the efficient properties admit a larger disparity for this phase. Note that the variation of the solid fraction of the aluminate phases can also impact the chemo-mechanical response, such as sulfate attack. The matrix (C-S-H) remains the phase whose uncertainties have the most impact on the estimated properties.

At mortar scale, the mortar variation is, first of all, induced by the ITZ volume fraction uncertainty. Patel et al. (2016) observed a low impact of the ITZ phase on the diffusion properties, which may call into question the main influence of the mortar homogenization scheme obtained. As reported by Göbel et al. (2017), the uncertainty of the cement paste parameters is magnified during the upscaling processes but, for the elastic and diffusion coefficients, their influences are

negligible compared to the ITZ uncertainty. The Biot properties are impacted by the porosity and the volume fraction of ITZ. Note that the ITZ porosity has been little studied in the literature that could have a strong impact on the overall properties, see Table C.8.

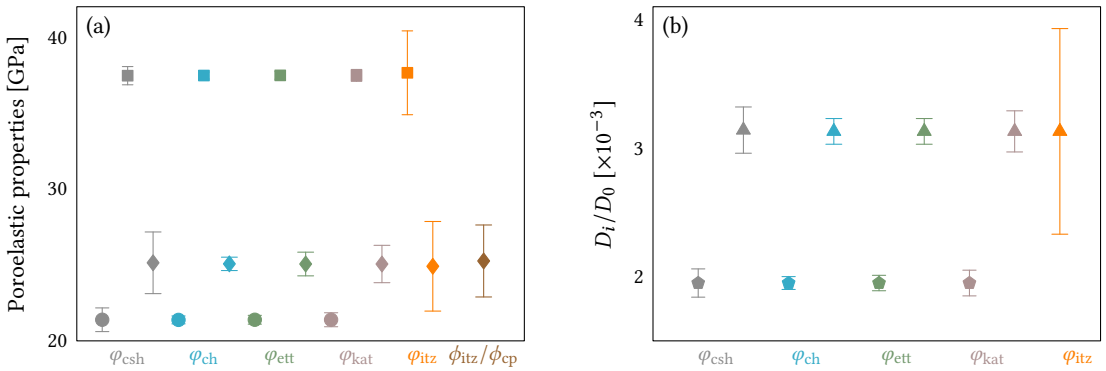

Figure 4 Uncertainty propagation from the microstructural properties (volume fractions and porosities). Mean value and standard deviation obtained through Monte-Carlo simulation are respectively represented by data symbols and error bars: (a) poroelastic properties and (b) normalized diffusion properties. Legend: ●E_{cp}, ■E_m, ♦$b_m N_m$, ⬟D_{cp}/D_0, and ▲D_m/D_0.

Main results The variations of poroelastic properties and diffusion coefficient increase with the volume fraction uncertainties of the inclusion and their impacts are magnified during the upscaling processes. The main sources of uncertainty at the cement paste and mortar scales remain respectively the C-S-H and ITZ properties.

4.3 Impact of all uncertainties

The impacts of material and microstructure uncertainties on the analytical estimated results are investigated. Based on the remarks of Stutzman et al. (2014) regarding the uncertainties associated with the Bogue formula rendering "supposedly distinct classes of cement practically indistinguishable", the homogenization propagation uncertainties are studied for three water-cement ratios.

The evolution of the apparent material properties is shown in Table 8 and plotted in Figure 5. The mean parameters follow the tendencies specified in the literature (experimental, numerical

w/c	E_{cp} [GPa]	E_m [GPa]	$b_m N_m$ [GPa]	$D_{cp}/D_0 \times 10^3$	$D_m/D_0 \times 10^3$
0.3	23.34 (±1.78)	38.07 (±6.54)	30.14 (±27.73)	1.44 (±0.8)	2.22 (±1.6)
0.4	18.92 (±1.51)	34.39 (±5.96)	32.54 (±23.03)	1.97 (±1.21)	3.04 (±2.8)
0.5	15.66 (±1.29)	31 (±5.68)	38.22 (±27.7)	2.55 (±1.4)	3.94 (±2.88)

Table 8 Input parameters, properties uncertainties study.

and analytical results): the diffusion increases and the Young Modulus decreases with the water-cement ratio (Bary and Béjaoui 2006; Béjaoui et al. 2006; Bernard and Kamali-Bernard 2012; Patel et al. 2016; Tognevi 2012). As previous results, the uncertainties increase with the mortar parameters, in particular the diffusion coefficients. Furthermore, the Biot coefficient evolution with the water-cement ratio is not clear.

The standard deviation increases with the upscaling due to the propagation of the uncertainties through the ITZ properties and volume fraction. The standard deviation of the diffusive properties decreases with the water-cement ratio that is in accordance with the results of Honorio et al. (2020a) for the conductivity properties of concrete material. We note an inverse tendency for the young modulus. These effects are relatively low and are more pronounced in (Honorio et al. 2020a). In our case, the volume fraction of the main inclusion (except the portlandite) and matrix remain quite similar but the capillary porosity increases due to the dissolution of the unreacted cement, see Table 1. The variation of the standard deviation with w/c can be due to the effect of the microstructural variability on the porosity which increases with the capillary porosity.

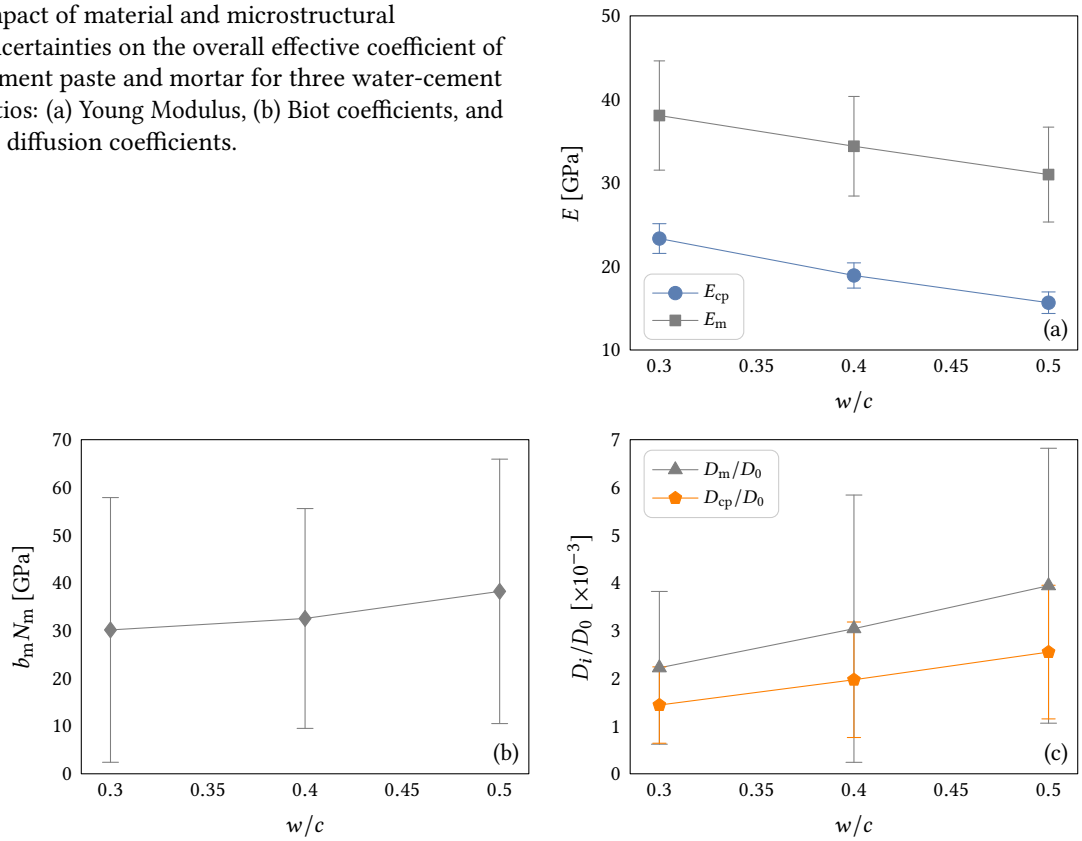

Figure 5 Impact of material and microstructural uncertainties on the overall effective coefficient of cement paste and mortar for three water-cement ratios: (a) Young Modulus, (b) Biot coefficients, and (c) diffusion coefficients.

The coefficient variation $V/\overline{e}$ is mainly impacted by the water-cement ratio and so for a low water-cement ratio, the predicted values admit a small error.

5 Sensitivity analysis

Section 4 highlights the impact of the morphologic and the material properties parameters in the global response. To identify the main contributor to the output variation, a sensitivity analysis study is carried out.

The sensitivity analysis is based on the variance-based method. The influences of each input are measured through the Sobol indices (between 0 and 1). The first order sensitivity Sobol index, denoted S_i, is used to measure the sensitivity of each input parameter:

$$S_i = \frac{V_{\mathbf{x}_i}(\overline{e}(\mathbf{y}|\mathbf{x}_i))}{V(\mathbf{y})}, \tag{13}$$

where $\mathbf{x}_i$ is the vector of input parameters, $\mathbf{y}$ is the output values given by the model, and i defines the input index. For more details, see (Gilquin et al. 2021; Saltelli 2002).

The system is computed using the Sobol-Saltelli method (Gilquin et al. 2021; Saltelli 2002; Venkovic et al. 2013; Sudret et al. 2010) where the Sobol indices are estimated through a Monte-Carlo experiments. Let us consider $\boldsymbol{X}^a \in \mathbb{R}^{N^i \times N^s}$ and $\boldsymbol{X}^b \in \mathbb{R}^{N^i \times N^s}$ two independent input sample matrices, where N^i and N^s are respectively the number of input values for each model and the number of Monte-Carlo samples. To compute the first order Sobol indices, a matrix, denoted $\boldsymbol{X}^{c,i}$, where all factors except the row j is equal to $\boldsymbol{X}^b$, is defined for each variable. The row i corresponds to the row of the matrix $\boldsymbol{X}^a$. The estimation of S_i is obtained by the products of the vector of output values estimated from $\boldsymbol{X}^a$ and each matrix $\boldsymbol{X}^{c,i}$, $\forall i \in N^i$, denoted respectively $\mathbf{y}^a$ and $\mathbf{y}^{c,i}$ (Gilquin et al. 2021; Saltelli 2002):

$$S_i' = \frac{\frac{1}{n}\sum_{j=1}^{n}(y_j^a \times y_j^{c,i}) - \left(\frac{1}{n}\sum_{j=1}^{n} y_j^a\right)^2}{\frac{1}{n}\sum_{j=1}^{n}(y_j^a)^2 - \left(\frac{1}{n}\sum_{j=1}^{n} y_j^a\right)^2}. \tag{14}$$

The first-order sensitivity indices measure only the direct effect of one parameter on the response of the micromechanical model. The total Sobol indices representing the interaction effect between parameters are estimated in the previous studies (Section 4.1 and Section 4.2). We focus here on the first order to distinguish the Sobol indices at the cement paste and at the mortar scales to highlight the highest Sobol index value. Moreover, the study allows us to consider the influence of the interaction effects of input properties on homogenized values. Only diffusive and elastic properties are considered because the Biot properties lead to high variation.

5.1 Analysis and results

Young Modulus Figure 6 shows the first order Sobol indices for the Young modulus of the cement paste and the mortar.

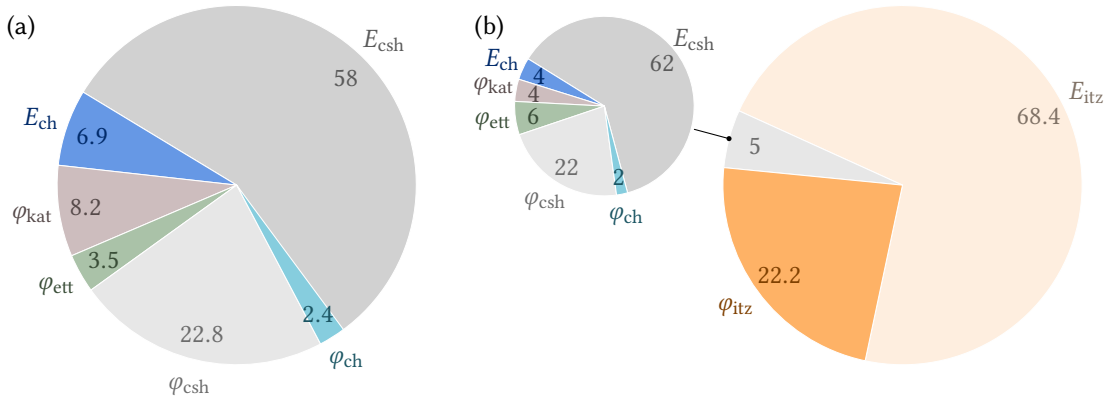

Figure 6 Sensitivity analysis of Young Modulus: first order Sobol indices of (a) cement paste and (b) mortar.

For the cement paste, the total sum of the indices is almost equals to 1, which means there are negligible interaction effects between the morphologic and the material properties. This result confirms the conclusion of the uncertainties studies. The C-S-H phases play a major role. The Young modulus must be estimated properly to simulate the elastic cement paste properties accurately. Furthermore, the viscoelastic properties of the cement paste, not studied here, are impacted by the C-S-H properties and volume fraction (Le 2011; Honorio et al. 2016; Sanahuja and Huang 2017). The aluminate phase (here the katoite) has a greater effect than the portlandite elastic properties and other morphological properties. Note that the uncertainties could be more important for the monosulfoaluminate phase because its Young Modulus is closed to that of Portlandite phase and it is greater than that of the katoite phase (Haecker et al. 2005). Nevertheless, the compressibility modulus value of the phase is still in debate, recent studies using the molecular simulations show the monosulfoaluminate properties are closed to that of the ettringite phase and thus the katoite (Honorio et al. 2020b). The volume fraction uncertainties are deduced from Bogue's equation (Stutzman et al. 2014). Hydration properties based on the total concentration of aluminates, instead of the mass fraction of C_3A (Papadakis et al. 1991; Tennis and Jennings 2000), could reduce the global uncertainties. The effect of other hydrates is negligible.

The mortar is impacted by the uncertainties associated with the ITZ phase. The total sum of the first order indices is 0.95 which highlights an impact negligible of the interaction between the variables. The main interaction is due to the ITZ strength, see Tables 5 and 7. The key parameter is the ITZ Young Modulus which is hard to deduce. From an experimental point of view, the identification of the microstructural and mechanical properties of the interphase remains a challenge (Jebli et al. 2018; Salah et al. 2019; Sun et al. 2007). Numerically, the representation of the ITZ phase (Honorio et al. 2016; Stora et al. 2009) can reduce the uncertainties, but additional variations can appear due to the material representativity. Such as the hydration, adding model parameters can increase the variation (Göbel et al. 2017). Furthermore, the ITZ strength properties depend on the aggregate and sand which impact the homogenized response (Keinde 2014). Our approach seems to be a convenient choice to consider the impact of the variation of ITZ elastic properties independently of the inclusion characteristics.

Diffusion coefficient Figure 7 shows the first order Sobol indices for the diffusion coefficient of the cement paste and the mortar.

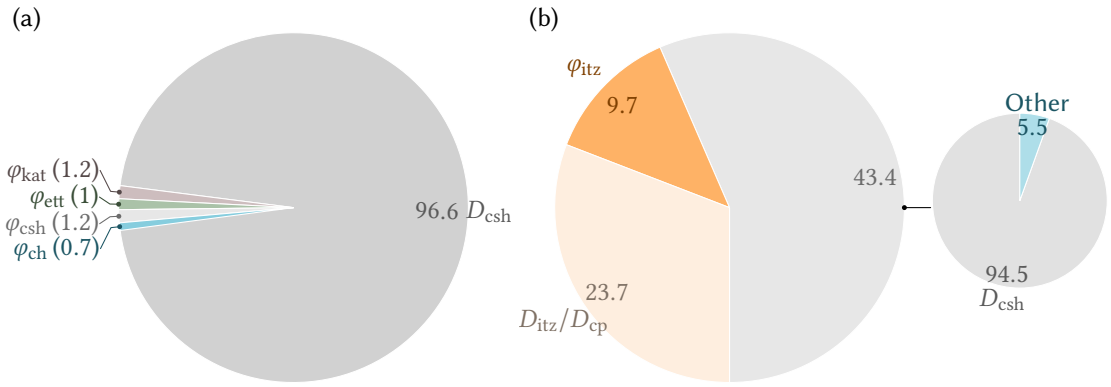

Figure 7 Sensitivity analysis of diffusion coefficient: first order Sobol indices of (a) cement paste and (b) mortar.

At cement paste scale, the interaction between the microstructure and the local diffusivity is negligible. The diffusivity depends essentially on the C-S-H diffusion. This result agrees with (Patel et al. 2016). Furthermore, distinguishing the C-S-H phases and identifying the diffusion coefficient for each phase remain an experimental challenge (Constantinides and Ulm 2004; Korb et al. 2007; Seigneur et al. 2017).

At mortar scale, the sum of the first Sobel indices highlights the main impact of the interaction term. The interaction is due to the upscaling impact of the cement paste volume fraction variation and the relationship between the ITZ and the cement paste diffusion properties. In the first order, the cement paste properties have the main effect on the homogenized coefficients. The effects of interaction and the C-S-H properties could be one of the major roles in the multi-scale model. The mortar is also mainly impacted by the uncertainties associated with the ITZ phase (volume fraction and diffusion coefficient). The three-coated homogenization scheme models the percolation of the transitional phase and thus the volume fraction is also a key parameter to estimate.

Main results This study highlighted the main sources of uncertainty of the model and the interaction between the model parameters. The interaction between the microstructure and material properties remains negligible except for the diffusion coefficient of the mortar. The main conclusion highlighted with the uncertainty study is confirmed in this study: the ITZ and C-S-H are the main parameters affecting the efficient properties. The effect of the C-S-H Young modulus is quite negligible at the mortar scale for the Young modulus compared to the ITZ parameters.

6 Conclusions

To study the chemo-mechanics behavior of concrete, a multi-scale microporomechanics model was proposed in (Socié 2019; Socié et al. 2019; Socié et al. 2021). The model allows to estimate the diffusive and poroelastic properties of mortar and to highlight the effect of the microstructural characteristic. The microporomechanical model is based on a representation at cement paste and mortar scales. The homogenization scheme follows the recommendations of the literature for a mature material.

The model was validated for various cement pastes and mortars by comparison with analytical homogenization models and experimental results. A probabilistic approach was applied to the multi-scale model to investigate the uncertainty propagation of the microstructural and material properties. The results highlighted the main impact of the cement matrix (C-S-H) uncertainties at the cement paste scale and the Interfacial Transition Zone at the mortar scale for the diffusive and the poroelastic properties. Based on (Stutzman et al. 2014), the influence of Bogue's uncertainties through the initial volume of each hydrated was investigated. Despite the C-S-H phases, the aluminate hydrate has a major impact on the poroelastic properties. The propagation of the global uncertainties for three water-cement ratios showed the ability of the model to capture the

effect of the material evolution on the diffusive and elastic properties. However, the uncertainties of the Biot parameters are too important to obtain quantitative estimation.

The last part of the paper was dedicated to a sensitivity analysis based on the first Sobol indices. This study highlighted the negligible interaction between the microstructure and the local diffusivity for the diffusive and elastic properties of the cement paste and for the mortar Young modulus. For a solid phase, the model was mainly dependent on the material properties rather than the volume fraction. For the Young modulus, the main conclusion of the uncertainty analysis was similar. The C-S-H was the main uncertainties input parameter at the cement paste scale and the ITZ, at the mortar scale. The cement paste was also impacted by the volume fraction of the aluminate phases and the effect of the portlandite phase remained negligible. For the diffusivity at the cement paste scale, the C-S-H was the main factor, in agreement with (Patel et al. 2016). For the mortar diffusivity term, the interaction between the input parameters and the C-S-H effect was predominant. The study underlined the predominant impact of the ITZ volume fraction and properties to estimate mortar properties.

Finally, the study highlighted the large variety of microstructures, due to the uncertainties associated to the Bogue formulation, that mainly impact the C-S-H and aluminate phases, which are the limiting reactant of the Delayed Ettringite Formation and External Sulphate Attack (Socié 2019). The results could be applied to a chemo-mechanical Finite Element simulation to consider the impact of the overall uncertainties on the chemical and mechanical degradation kinetics.

A Uncertainties associated to the hydration model

Bogue's formula (Bogue 1929; Taylor 1989; Stutzman et al. 2014) is used to estimate the main cement phases from the clinker chemical properties. Stutzman et al. (2014) studied the impact of the uncertainties associated with the formula. According to the authors, the uncertainties associated with the Bogue formula have a great impact on the microstructure and material properties estimated by the hydration model. Indeed, the main cement phases C_2S, C_3S, C_3A and C_4AF are commonly used in the hydration model to predict the initial concrete properties (Bary et al. 2014; Jennings and Tennis 1994; Tennis and Jennings 2000). To study the impact of the Bogue model uncertainties on the poroelastic and diffusive properties, a Monte-Carlo method is carried out on the hydration model developed in (Socié 2019). The hydration model differs from the one used by Bary and Béjaoui (2006); Tognevi (2012), which is the model of Tennis and Jennings (2000), because it is applied for a mature concrete and a totally hydrated reaction is assumed. The cement paste microstructure is estimated by a thermodynamical chemical model developed in (Socié et al. 2021). This methodology is mainly used and validated in reactive transport (De Windt and Devillers 2010; Planel 2002; Seigneur et al. 2020). The article focuses on the role of the microstructure uncertainties and the material properties on the analytical homogenization results. Our study rests on the microstructure from (Bary and Béjaoui 2006). The hydration model of Socié (2019) is considered to estimate the uncertainties propagation reported in (Stutzman et al. 2014). The comparison of different hydration models achieved in (Göbel et al. 2017; Honorio et al. 2020a; Venkovic et al. 2013) could form an extension of the present study.

The total concentration of each main component is estimated on the mass fraction of each component of the clinker, denoted f_i^m for the solid i, and the water-cement mass ratio w/c:

$$\begin{aligned}
(C^{aq}_{tot})_{Ca^{2+}} &= 3C_{C_3S} + 2C_{C_2S} + 3C_{C_3A} + C_{CaSO_4} + 4C_{C_4AF}\\
(C^{aq}_{tot})_{H_2SiO_4^{2-}} &= C_{C_3S} + C_{C_2S}\\
(C^{aq}_{tot})_{SO_4^{2-}} &= C_{CaSO_4}\\
(C^{aq}_{tot})_{Al(OH)_4^-} &= 2C_{C_3A} + 2C_{C_4AF},
\end{aligned} \tag{A.1}$$

with (Planel 2002):

$$m_{ci} = \frac{V_{\text{total}}\rho_{ci}}{\frac{w}{c}\frac{\rho_{ci}}{\rho_w} + 1}; \quad (C^{aq}_{tot})_i = \frac{M_i f_i^m m_{ci}}{V_{\text{total}}}, \quad \forall i \in [1,4] \tag{A.2}$$

where i is the species with corresponding molar mass M_i [kg mol^{-1}], cement mass m_{ci} [kg], cement density ρ_{ci} [kg m^{-3}]; also ρ_w is the water density [kg m^{-3}] and V_{total} is the total volume [m^3].

The thermodynamic chemical solver (Socié et al. 2021) gives the concentration of each main phase of the cement phases and the molar fractions are simply deduced by multiplying the concentration by the molar volume. A Monte-Carlo scheme is carried out on the results of Stutzman et al. (2014), see Table A.1, using a log-normal distribution for each phase. Furthermore,

	C_3S	C_2S	C_3A	C_4AF	Gypsum
Mass fraction (%)	58.4 ± 9.72	14.5 ± 9.68	9.9 ± 2.6	7.1 ± 1.56	6.1

Table A.1 Mass fraction used, based on the cement paste used in (Planel et al. 2006), with a water cement ratio of 0.4. The standard deviation is based on (Stutzman et al. 2014).

the C-S-H molar volume is hard to measure because it depends on the type of C-S-H (Tennis and Jennings 2000) as well as the calcium silica ratio of the phase (Stora et al. 2009). We study two values of C-S-H and the other molar volumes are summarized in Table A.2. The results are

Chemical equations			$\log_{10}(K^{sol})$	Molar volume [m^3 mol^{-1}]
C-S-H(1.65)	⇔	$1.65Ca^{2+} + 3.3OH^- + SiO_2 - 2H_2O$	−17.64	0.084, 0.078
Portlandite	⇔	$Ca^{2+} + 2OH^-$	−5.19	0.033
Katoite	⇔	$2Al(OH)_4^- + 3Ca^{2+} + 4OH^-$	−20.5	0.707
Ettringite	⇔	$2Al(OH)_4^- + 6Ca^{2+} + 3SO_4^{2-} + 4OH^- + 26H_2O$	−44.9	0.15

Table A.2 Hydrate properties considered in the hydration model: chemical reactions, dissolution equilibrium constants $\log_{10}(K^{sol})$, and molar volumes (Planel 2002; Lothenbach et al. 2019).

summarized in Table A.3. The solid aluminate phase, here the katoite, and the C-S-H area are impacted by the variation.

Phases	C-S-H	Portlandite	Ettringite	Katoite
Volume fraction	0.374 ± 0.018	0.184 ± 0.005	0.144 ± 0.007	0.07 ± 0.011

Table A.3 Results obtained via the hydration computation.

B C-S-H diffusion coefficient

The C-S-H diffusion coefficient used in the literature are listed in Table B.4. In case of two C-S-H phases, the C-S-H homogenized value is estimated using the Maxwell scheme. Note that we do not include the following values 19.4×10^{-12} m^2 s^{-1} (Bogdan 2015) and 25×10^{-12} m^2 s^{-1} (Seigneur et al. 2017) because theses values are well beyond the mean value found in the literature. We find the mean value and standard deviation $4.64 \pm 2.84 \times 10^{-12}$.

Table B.4 C-S-H diffusion coefficient D_{csh} used in the literature. In case of articles using two C-S-H phases, the homogenized value is estimated using Maxwell scheme.

D_{csh} [10^{-12} m^2 s^{-1}]	References
2.2	Bernard and Kamali-Bernard (2012)
3.2	Bary (2008)
5.097	Stora et al. (2009)
5.97, 1.23, 4, 2.66, 2.9	Patel et al. (2016)
8	Socié (2019)
11	Korb et al. (2007)

C Mortar uncertainties

The section lists the ITZ property values used or measured in the literature.

Table C.5 ITZ diffusion coefficient D_{itz}/D_{cp} used in the literature.

D_{itz}/D_{cp}	References
4	Bogdan (2015); Kamali-Bernard et al. (2009)
12.5	Nilenius et al. (2014)
20.7	Patel et al. (2016)

Table C.6 ITZ Young modulus coefficient E_{itz}/E_{cp} used in the literature.

E_{itz}/E_{cp}	References
0.2	Stora (2007)
0.4	Heukamp (2003)
0.5	Hashin and Monteiro (2002); Garboczi (1997)
0.66	Tognevi (2012)
0.76	Honorio et al. (2016)
0.74	Kamali-Bernard et al. (2009)
[0.1, 0.9]	Keinde (2014)

Table C.7 ITZ volume fraction φ_{itz} used in the literature.

φ_{itz}	References
0.09	Bary et al. (2014)
0.104	Stora et al. (2009)
0.2	Honorio et al. (2016); Socié (2019)
0.217	Stora et al. (2009)
0.3	Heukamp (2003)

Table C.8 ITZ porosity ϕ_{itz}/ϕ used in the literature.

ϕ_{itz}/ϕ	References
[1.5, 2]	Keinde (2014)
[1.5, 4]	Kamali-Bernard et al. (2009)
1.5	Patel et al. (2016)

References

Aït-Mokhtar, A., R. Belarbi, F. Benboudjema, N. Burlion, B. Capra, M. Carcassès, J.-B. Colliat, F. Cussigh, F. Deby, F. Jacquemot, T. de Larrard, J.-F. Lataste, P. Le Bescop, M. Pierre, S. Poyet, P. Rougeau, T. Rougelot, A. Sellier, J. Séménadisse, J.-M. Torrenti, A. Trabelsi, P. Turcry, and H. Yanez-Godoy (2013). Experimental investigation of the variability of concrete durability properties. *Cement and Concrete Research* 45:21–36. [DOI], [HAL].

Bary, B. (2008). Simplified coupled chemo-mechanical modeling of cement pastes behavior subjected to combined leaching and external sulfate attack. *International Journal for Numerical and Analytical Methods in Geomechanics* 32(14):1791–1816. [DOI].

Bary, B. and S. Béjaoui (2006). Assessment of diffusive and mechanical properties of hardened cement pastes using a multi-coated sphere assemblage model. *Cement and Concrete Research* 36(2):245–258. [DOI], [HAL].

Bary, B., N. Leterrier, E. Deville, and P. Le Bescop (2014). Coupled chemo-transport-mechanical modelling and numerical simulation of external sulfate attack in mortar. *Cement and Concrete Composites* 49:70–83. [DOI], [HAL].

Bernard, F. and S. Kamali-Bernard (2012). Predicting the evolution of mechanical and diffusivity properties of cement pastes and mortars for various hydration degrees – A numerical simulation investigation. *Computational Materials Science* 61:106–115. [DOI].

Bogdan, M. (2015). Morphological multisscale modeling of cementitious materials - Application to effective diffusive properties prediction. PhD thesis. France: École Normale Supérieure de Cachan. [HAL].

Bogue, R. (1929). Calculation of the Compounds in Portland Cement. *Industrial & Engineering Chemistry Analytical Edition* 1(4):192–197. [DOI].

Bourdette, B. (1994). Durabilité du mortier, prise en compte des auréoles de transition dans la caractérisation et la modélisation des processus physiques et chimiques d'altération. French. PhD thesis. France: INSA Toulouse.

Buffo-Lacarrière, L., A. Sellier, G. Escadeillas, and A. Turatsinze (2007). Multiphasic finite element

modeling of concrete hydration. *Cement and Concrete Research* 37(2):131–138. [DOI], [HAL].

Béjaoui, S. and B. Bary (2007). Modeling of the link between microstructure and effective diffusivity of cement pastes using a simplified composite model. *Cement and Concrete Research* 37(3):469–480. [DOI], [HAL].

Béjaoui, S., B. Bary, S. Nitsche, D. Chaudanson, and C. Blanc (2006). Experimental and modeling studies of the link between microstructure and effective diffusivity of cement pastes. *Revue Européenne de Génie Civil* 10(9):1073–1106. [DOI], [HAL].

Constantinides, G. and F.-J. Ulm (2004). The effect of two types of C-S-H on the elasticity of cement-based materials: Results from nanoindentation and micromechanical modeling. *Cement and Concrete Research* 34(1):67–80. [DOI], [HAL].

De Windt, L. and P. Devillers (2010). Modeling the degradation of Portland cement pastes by biogenic organic acids. *Cement and Concrete Research* 40(8):1165–1174. [DOI].

Dormieux, L., D. Kondo, and F.-J. Ulm (2006). *Microporomechanics*. Wiley. ISBN: 9780470031995.

El-Hachem, R., E. Rozière, F. Grondin, and A. Loukili (2012). Multi-criteria analysis of the mechanism of degradation of Portland cement based mortars exposed to external sulphate attack. *Cement and Concrete Research* 42(10):1327–1335. [DOI], [HAL].

Gallé, C., H. Peycellon, and P. Le Bescop (2004). Effect of an accelerated chemical degradation on water permeability and pore structure of cement-based materials. *Advances in Cement Research* 16(3):105–114. [DOI].

Garboczi, E. (1997). Stress, displacements, and expansive cracking around a single spherical aggregate under different expansive conditions. *Cement and Concrete Research* 27(4):495–500. [DOI].

Garboczi, E. and D. Bentz (1997). Analytical formulas for interfacial transition zone properties. *Advanced Cement Based Materials* 6(3-4):99–108. [DOI].

Gilquin, L., C. Prieur, Arnaud, and H. Monod (2021). Iterative estimation of Sobol' indices based on replicated designs. *Computational and Applied Mathematics* 40(1). [DOI], [HAL].

Göbel, L., T. Lahmer, and A. Osburg (2017). Uncertainty analysis in multiscale modeling of concrete based on continuum micromechanics. *European Journal of Mechanics - A/Solids* 65:14–29. [DOI].

Haecker, C.-J., E. Garboczi, J. Bullard, R. Bohn, Z. Sun, S. Shah, and T. Voigt (2005). Modeling the linear elastic properties of Portland cement paste. *Cement and Concrete Research* 35(10):1948–1960. [DOI], [HAL].

Hajilar, S. and B. Shafei (2015). Nano-scale investigation of elastic properties of hydrated cement paste constituents using molecular dynamics simulations. *Computational Materials Science* 101:216–226. [DOI].

Hashin, Z. and P. Monteiro (2002). An inverse method to determine the elastic properties of the interphase between the aggregate and the cement paste. *Cement and Concrete Research* 32(8):1291–1300. [DOI].

Heukamp, F. (2003). Chemomechanics of Calcium Leaching of Cement-Based Materials at Different Scales: The Role of CH-Dissolution and C-S-H Degradation on Strength and Durability Performance of Materials and Structures. PhD thesis. USA: Massachusetts Institute of Technology. [HDL].

Honorio, T., B. Bary, and F. Benboudjema (2016). Multiscale estimation of ageing viscoelastic properties of cement-based materials: A combined analytical and numerical approach to estimate the behaviour at early age. *Cement and Concrete Research* 85:137–155. [DOI].

Honorio, T., H. Carasek, and O. Cascudo (2020a). Electrical properties of cement-based materials: Multiscale modeling and quantification of the variability. *Construction and Building Materials* 245:118461. [DOI].

Honorio, T., P. Guerra, and A. Bourdot (2020b). Molecular simulation of the structure and elastic properties of ettringite and monosulfoaluminate. *Cement and Concrete Research* 135:106126. [DOI].

Jebli, M., F. Jamin, E. Malachanne, E. Garcia-Diaz, and M. El Youssoufi (2018). Experimental characterization of mechanical properties of the cement-aggregate interface in concrete. *Construction and Building Materials* 161:16–25. [DOI], [HAL].

Jelea, A. (2018). On the Laplace-Young equation applied to spherical fluid inclusions in solid

matrices. *Journal of Nuclear Materials* 505:127–133. [DOI], [HAL].

Jennings, H. and P. Tennis (1994). Model for the developing microstructure in Portland cement pastes. *Journal of the American Ceramic Society* 77(12):3161–3172. [DOI].

Kamali-Bernard, S., F. Bernard, and W. Prince (2009). Computer modelling of tritiated water diffusion test for cement based materials. *Computational Materials Science* 45(2):528–535. [DOI].

Keinde, D. (2014). Etude du béton à l'échelle mésoscopique : simulation numérique et tests de micro-indentation. French. PhD thesis. France: INSA Rennes. [HAL].

Korb, J.-P., L. Monteilhet, P. McDonald, and J. Mitchell (2007). Microstructure and texture of hydrated cement-based materials: A proton field cycling relaxometry approach. *Cement and Concrete Research* 37(3):295–302. [DOI].

Le, Q. V. (2011). Modélisation multi-échelle des matériaux viscoélastiques hétérogènes : application à l'identification et à l'estimation du fluage propre d'enceintes de centrales nucléaires. French. PhD thesis. France: Université Paris-Est. [HAL].

Le Bellégo, C. (2001). Couplages chimie-mécanique dans les structures en béton attaquées par l'eau : Étude expérimentale et analyse numérique. French. PhD thesis. France: École Normale Supérieure de Cachan.

Le Bellégo, C., G. Pijaudier-Cabot, B. Gérard, J.-F. Dubé, and L. Molez (2003). Coupled mechanical and chemical damage in calcium leached cementitious structures. *Journal of Engineering Mechanics* 129(3):333–341. [DOI], [HAL].

Lothenbach, B., D. Kulik, T. Matschei, M. Balonis, L. Baquerizo, B. Dilnesa, G. Miron, and R. Myers (2019). Cemdata18: A chemical thermodynamic database for hydrated Portland cements and alkali-activated materials. *Cement and Concrete Research* 115:472–506. [DOI], [OA].

Mori, T. and K. Tanaka (1973). Average stress in matrix and average elastic energy of materials with misfitting inclusions. *Acta Metallurgica* 21(5):571–574. [DOI].

Nguyen, N., A. Giraud, and D. Grgic (2011). A composite sphere assemblage model for porous oolitic rocks. *International Journal of Rock Mechanics and Mining Sciences* 48(6):909–921. [DOI].

Nguyen, T. (2010). Apport de la modélisation mésoscopique dans la prédiction des écoulements dans les ouvrages en béton fissuré en conditions d'accident grave. French. PhD thesis. France: Université de Pau et des Pays de l'Adour. [HAL].

Nilenius, F., F. Larsson, K. Lundgren, and K. Runesson (2014). Computational homogenization of diffusion in three-phase mesoscale concrete. *Computational Mechanics* 54:461–472. [DOI], [OA].

Papadakis, V., C. Vayenas, and M. Fardis (1991). Physical and chemical characteristic affecting the durability of concrete. *ACI Materials Journal* 2(88):186–196. [HAL].

Patel, R., Q. Phung, S. Seetharam, J. Perko, D. Jacques, N. Maes, G. De Schutter, G. Ye, and K. Van Breugel (2016). Diffusivity of saturated ordinary Portland cement-based materials: A critical review of experimental and analytical modelling approaches. *Cement and Concrete Research* 90:52–72. [DOI].

Planel, D. (2002). Les effets couplés de la précipitation d'espèces secondaires sur le comportement mécanique et la dégradation chimique des bétons. French. PhD thesis. France: Université de Marne la Vallée. [HAL].

Planel, D., J. Sercombe, P. Le Bescop, F. Adenot, and J.-M. Torrenti (2006). Long-term performance of cement paste during combined calcium leaching–sulfate attack: kinetics and size effect. *Cement and Concrete Research* 36(1):137–143. [DOI].

Salah, N., M. Jebli, E. Malachanne, F. Jamin, F. Dubois, A.-S. Caro, E. Garcia-Diaz, and M. El Youssoufi (2019). Identification of a cohesive zone model for cement paste-aggregate interface in a shear test. *European Journal of Environmental and Civil Engineering*, 1–15. [DOI], [HAL].

Saltelli, A. (2002). Making best use of model evaluations to compute sensitivity indices. *Computer Physics Communications* 145(2):280–297. [DOI], [HAL].

Sanahuja, J. and S. Huang (2017). Mean-field homogenization of time-evolving microstructures with viscoelastic phases: application to a simplified micromechanical model of hydrating cement paste. *Journal of Nanomechanics and Micromechanics* 7(1):04016011. [DOI], [HAL].

Seigneur, N., E. Kangni-Foli, V. Lagneau, A. Dauzères, S. Poyet, P. Le Bescop, E. L'Hôpital, and

J.-B. d'Espinose de Lacaillerie (2020). Predicting the atmospheric carbonation of cementitious materials using fully coupled two-phase reactive transport modelling. *Cement and Concrete Research* 130:105966. [DOI], [HAL].

Seigneur, N., E. L'Hôpital, A. Dauzères, J. Sammaljavi, M. Voutilainen, P. Labeau, A. Dubus, and V. Detilleux (2017). Transport properties evolution of cement model system under degradation - Incorporation of a pore-scale approach into reactive transport modelling. *Physics and Chemistry of the Earth, Parts A/B/C* 99:95–109. [DOI].

Socié, A. (2019). Modélisation chimio-mécanique de la fissuration de matériaux cimentaires : vieillissement et tenue des enceintes de confinement des centrales nucléaires. French. PhD thesis. France: Université de Montpellier. [HAL].

Socié, A., F. Dubois, Y. Monerie, and F. Perales (2021). Multibody approach for reactive transport modeling in discontinuous-heterogeneous porous media. *Computational Geosciences* 25(5):1473–1491. [DOI], [HAL].

Socié, A., F. Perales, F. Dubois, and Y. Monerie (2019). Chemo-poro-mechanical modeling of cementitious materials (diffusion-precipitation-cracking). International Conference on Sustainable Materials, Systems and Structures (Rovinj, Croatia, Mar. 20, 2019–Mar. 22, 2019), pp 23–30. [HAL].

Stora, E. (2007). Multi-scale modelling and simulations of the chemo-mechanical behavior of degraded cement-based materials. PhD thesis. France: Université Paris-Est. [HAL].

Stora, E., B. Bary, Q.-C. He, E. Deville, and P. Montarnal (2009). Modelling and simulations of the chemo–mechanical behaviour of leached cement-based materials: Leaching process and induced loss of stiffness. *Cement and Concrete Research* 39(9):763–772. [DOI].

Stutzman, P., A. Heckert, A. Tebbe, and S. Leigh (2014). Uncertainty in Bogue-calculated phase composition of hydraulic cements. *Cement and Concrete Research* 61-62:40–48. [DOI].

Sudret, B., T. Yalamas, E. Noret, and P. Willaume (2010). Sensitivity analysis of nested multi-physics models using polynomial chaos expansions. *Safety, Reliability and Risk of Structures, Infrastructures and Engineering Systems.* 10th International Conference on Structural Safety and Reliability (Osaka, Japan, Sept. 13, 2009–Sept. 17, 2009). [HAL].

Sun, Z., E. Garboczi, and S. Shah (2007). Modeling the elastic properties of concrete composites: Experiment, differential effective medium theory, and numerical simulation. *Cement and Concrete Composites* 29(1):22–38. [DOI].

Taylor, H. F. W. (1989). Modification of the Bogue calculation. *Advances in Cement Research* 2(6):73–77. [DOI].

Tennis, P. and H. Jennings (2000). A model for two types of calcium silicate hydrate in the microstructure of Portland cement pastes. *Cement and Concrete Research* 30(6):855–863. [DOI], [HAL].

Tognevi, A. (2012). Modélisation multi-échelle et simulation du comportement thermo-hydro-mécanique du béton avec représentation explicite de la fissuration. French. PhD thesis. France: École Normale Supérieure de Cachan. [HAL].

Ulm, F.-J., G. Constantinides, and F. Heukamp (2004). Is concrete a poromechanics material?-A multiscale investigation of poroelastic properties. *Materials and Structures* 37:43–58. [DOI], [HAL].

Venkovic, N., L. Sorelli, B. Sudret, T. Yalamas, and R. Gagné (2013). Uncertainty propagation of a multiscale poromechanics-hydration model for poroelastic properties of cement paste at early-age. *Probabilistic Engineering Mechanics* 32:5–20. [DOI], [HAL].

Authors' contributions A.S: Conceptualization, Methodology, Validation, Analysis, Visualization, Writing original draft, Review and Editing. Y.M.: Conceptualization, Methodology, Analysis, Visualization, Writing, Review and Editing, Supervision. F.P.: Methodology, Analysis, Writing, Review and Editing, Supervision.

Supplementary Material None.

Acknowledgements Authors would like to thank Jean Baccou for his help and advice for the sensitivity analysis.

Ethics approval and consent to participate Not applicable.

Consent for publication Not applicable.

Competing interests The authors declare that they have no competing interests.

Journal's Note JTCAM remains neutral with regard to the content of the publication and institutional affiliations.